3D-QSAR and docking study on 3-benzimidazol-2-ylhydroquinolin-2-one derivatives as VEGFR-2 tyrosine kinase inhibitors

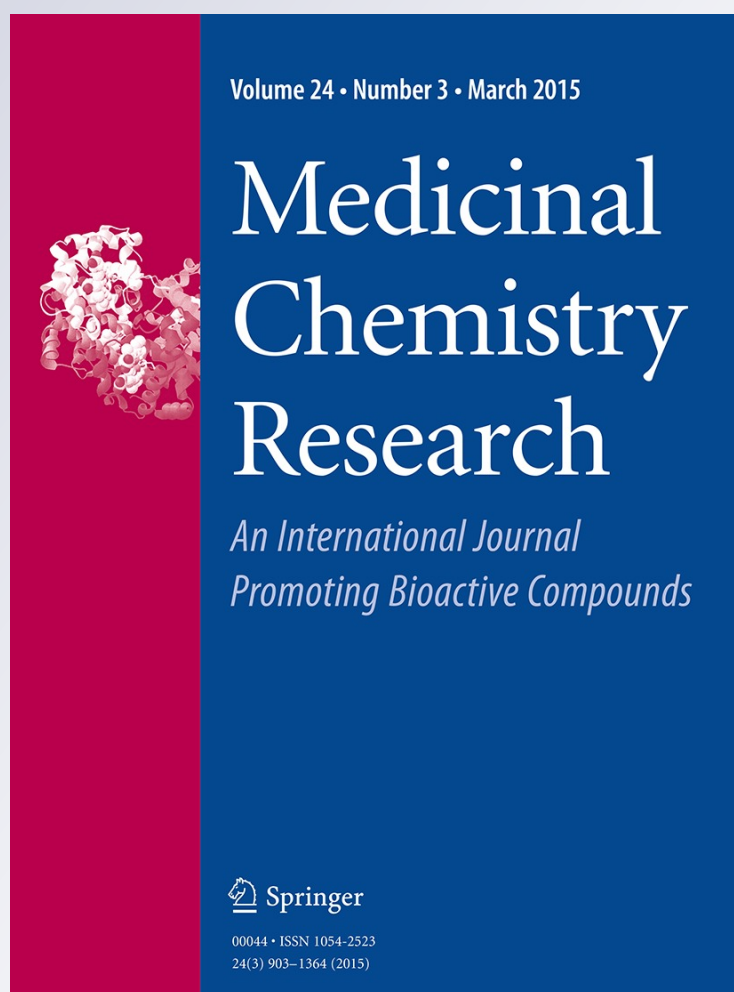Cong-min Kang, Dong-qing Liu, Xin-yu Wang, Ying-jie Dai, Jia-gao Cheng & Ying-tao Lv

Springer

Springer

ORIGINAL RESEARCH

3D-QSAR and docking study on 3-benzimidazol-2-ylhydroquinolin-2-one derivatives as VEGFR-2 tyrosine kinase inhibitors

Cong-min Kang · Dong-qing Liu · Xin-yu Wang ·
Ying-jie Dai · Jia-gao Cheng · Ying-tao Lv

Abstract The present study is an attempt to formulate the three-dimensional quantitative structure–activity relationship (3D-QSARs) modeling of 3-benzimidazol-2-ylhydroquinolin-2-one derivatives inhibiting vascular endothelial growth factor receptor-2 (VEGFR-2) tyrosine kinase. The 3D-QSARs were established for 36 3-benzimidazol-2-ylhydroquinolin-2-one derivatives as VEGFR-2 tyrosine kinase inhibitors using comparative molecular field analysis (CoMFA) and comparative similarity indices analysis (CoMSIA) techniques. The negative logarithm of IC_{50} (pIC_{50}) was used as the biological activity in the 3D-QSAR study. With the CoMFA model, the cross-validated value (q^2) was 0.516, the non-cross-validated value (R^2) was 0.927, and the external cross-validated value (Q_{ext}^2) was 0.855; with the CoMSIA model, the corresponding q^2, R^2, and Q_{ext}^2 values were 0.538, 0.980, and 0.809, respectively. The CoMFA and CoMSIA models were validated by a structurally diversified test set of nine compounds. Then, molecular docking was carried out to better understand of the interactions between VEGFR-2 tyrosine kinase target and inhibitors. Finally, based on results of the structure–activity relationship and of the molecular docking, seven VEGFR-2 tyrosine kinase inhibitors that showed excellent potencies have been constructed.

C. Kang · D. Liu · X. Wang · Y. Dai · Y. Lv (✉)
College of Chemical Engineering, Qingdao University
of Science and Technology, Qingdao 266042,
People's Republic of China
e-mail: lvyingtao@qust.edu.cn

J. Cheng
Shanghai Key Laboratory of Chemical Biology, School of
Pharmacy, East China University of Science and Technology,
Shanghai 200237, People's Republic of China

Introduction

Angiogenesis and maintenance of newly formed blood vessels are important normal physiological processes, and are also utilized by cancer to promote their survival, growth, and metastasis. A subset of growth factors and their receptor tyrosine kinases is the key signaling molecules during angiogenesis and vascular maintenance (Carmeliet, 2000; Doi et al., 2013). Among these growth factors, vascular endothelial growth factor (VEGF) and its receptors (VEGFR), especially VEGFR-2, play key roles in angiogenesis (Shibuya, 2013). VEGF is considered most important for both normal and pathological angiogenesis, and VEGFR-2 is the most dominant player (Cai et al., 2008; Ramsden, 2000). Inhibition of VEGFR-2 tyrosine kinase has been shown to suppress both angiogenesis and tumor growth in vivo (Jeltsch et al., 2013). Consequently, various VEGFR-2 tyrosine kinase inhibitors, including receptor-specific antibodies and low-molecular-weight chemicals such as sorafenib, vandetanib, sunitinib, and telatinib, have recently been developed (Bhargava and Robinson, 2011; Ding et al., 2013; Lee et al., 2012; Steeghs et al., 2011).

Nowadays, 3D-QSAR techniques (Gupta et al., 2014), such as comparative molecular field analysis (CoMFA) (Cramer et al., 1988) and comparative molecular similarity indices analysis (CoMSIA) (Böhm et al., 1999; Klebe et al., 1994) are routinely used in modern drug design to help in understanding drug–target interaction. These computational techniques have been proved particularly helpful in the design of novel, more potent inhibitors by revealing the mechanism of drug–target interaction (Xiao et al.,

2008). Here, we present 3D-QSAR studies using CoMFA and CoMSIA methods on 3-benzimidazol-2-ylhydroquinolin-2-one derivatives as VEGFR-2 tyrosine kinase inhibitors by considering the steric, electrostatic, and hydrophobic influences. The selected ligands were docked into the binding site of the three-dimensional model of VEGFR-2 tyrosine kinase using AutoDock software, and possible interaction models between VEGFR-2 tyrosine kinase and its inhibitors were obtained.

Materials and methods

Datasets for analysis

In this study, a dataset of 36 compounds obtained from Renhowe *et al*.'s work consisted of 3-benzimidazol-2-ylhydroquinolin-2-one derivatives which showed inhibitory activity toward human recombinant protein of VEGFR-2 (Renhowe *et al*., 2009). The general chemical structures and biological activity values of all small molecules are shown in Table 1. In the total set of the 36 compounds reported, 27 compounds were used as a training set, and the remaining 9 compounds labeled with "*" were used as a test set, based on a random selection. The IC_{50} values were converted into the corresponding pIC_{50} ($-lgIC_{50}$) and used as dependent variables in CoMFA and CoMSIA analysis. Three-dimensional structure building and all modeling were performed using the Sybyl 7.2 program package (Tripos Inc., St. Louis, USA).

Minimization and alignment

Molecular structures were sketched with sketch module in SYBYL and minimized using Tripos force field (Clark *et al*., 1989) with the Gasteiger–Huckel charges and conjugated gradient method, and gradient convergence criteria of 0.01 kcal/mol. Simulated annealing on the energy minimized structures was performed with 20 cycles. They were heated at 1,000 K for 1,000 fs to reach the equilibrium and annealed to 300 K for 1,500 fs. 36 conformations were then minimized to get low-energy conformations for each compound. The training set was aligned using align database. The most active compound (compound **20**) was used as an alignment template and the rest of the training set was aligned to it using the common substructure as shown in Fig. 1. The superimposed structures of aligned training set are shown in Fig. 2.

CoMFA and CoMSIA procedures

Based on the molecular alignment, CoMFA and CoMSIA studies were performed on these inhibitors to analyze the specific contributions of steric, electrostatic, and hydrophobic

effects to the bioactivities of the inhibitors. CoMFA calculates steric and electrostatic properties according to Lennard-Jones and Coulomb potentials, respectively, whereas CoMSIA calculates the similarity indices in the space surrounding each of the molecules in the dataset.

CoMFA steric and electrostatic interaction fields were calculated at each lattice intersection point of a regularly spaced grid of 2.0 Å. The default value of 30 kcal/mol was set as a maximum steric and electrostatic energy cutoff. With standard options for scaling of variables, the regression analysis was carried out using the full cross-validated partial least squares (PLS) method (leave-one-out) (Bush and Nachbar, 1993; CramerS, 1993; McIntosh *et al*., 1996; Wold *et al*., 2001). The minimum sigma (column filtering) was set to 2.0 kcal/mol to improve the signal-to-noise ratio by omitting those lattice points whose energy variation was below this threshold. The final model, non-cross-validated conventional analysis, was developed with the optimum number of components to yield a non-cross-validated R^2 value.

In CoMSIA, a distance-dependent Gaussian-type physicochemical property has been adopted to avoid singularities at the atomic positions and dramatic changes of potential energy for grids being in the proximity of the surface. With the standard parameters and no arbitrary cutoff limits, five fields associated to five physicochemical properties, namely steric, electrostatic, and hydrophobic effects and hydrogen bond donor and acceptor were calculated. The steric contribution was reflected by the third power of the atomic radii of the atoms. The electrostatic descriptors are derived from atomic partial charges, the hydrophobic fields are derived from atom-based parameters developed by Viswanadhan and the hydrogen bond donor and acceptor indices are obtained by a rule-based method derived from experimental values (Viswanadhan *et al*., 1989).

PLS analysis

Partial least squares statistical method used in deriving the 3D-QSAR models is an extension of multiple regression analysis in which the original variables are replaced by a small set of their linear combinations. PLS method with leave-one-out (LOO) cross-validation was used in this study to determine the optimal numbers of components using cross-validated coefficient q^2. The external validation of various models was performed using a test set of nine molecules. The final analysis (non-cross-validated analysis) was carried out using the optimum number of components obtained from the cross-validation analysis to get correlation coefficient (R^2). The q^2 value determines the internal predictive ability of the model while r^2 value evaluates the internal consistency of the model. Thus, the best QSAR model was chosen on the basis of a combination of q^2 and R^2.

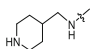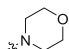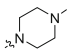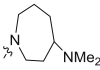**Table 1** Structures and activities of 36 3-benzimidazol-2-ylhydroquinolin-2-one derivatives
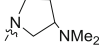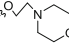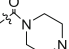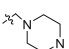
Comp.	R_1	R_4	R5′	R6′	pIC50		
					Exper	CoMFA	CoMSIA
1*	H	OH	H	H	6.62	6.47	6.39
2	CH$_3$	OH	H	H	5.24	5.50	5.22
3*	H	H	H	H	5.77	5.89	6.18
4	H	NH$_2$	H	H	7.24	7.01	6.89
5*	H	NHCH$_3$	H	H	6.66	6.38	6.39
6	H	N(CH$_3$)$_2$	H	H	6.07	6.11	6.09
7	H	(structure: HN-piperidinyl-methyl-NH)	H	H	6.03	6.07	6.13
8	H	NH$_2$	CH$_3$	CH$_3$	6.68	6.56	6.61
9	H	NH$_2$	CH$_3$	H	6.66	6.79	6.95
10*	H	NH$_2$	(structure: morpholine)	H	7.24	6.88	7.02
11	H	NH$_2$	(structure: N-methylpiperazine)	H	7.38	7.20	7.41
12	H	NH$_2$	(structure: azepane-NMe$_2$)	H	7.18	7.19	7.21
13	H	NH$_2$	(structure: pyrrolidine-NMe$_2$)	H	7.22	7.34	7.25
14*	H	NH$_2$	(structure: O-CH$_2$-morpholine)	H	7.18	7.43	7.54
15	H	NH$_2$	(structure: carbonyl-N-methylpiperazine)	H	7.59	7.69	7.73
16	H	NH$_2$	(structure: CH$_2$-N-methylpiperazine)	H	7.57	7.74	7.62

Table 1 continued
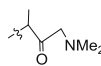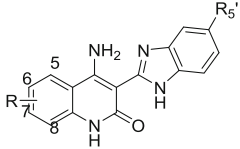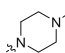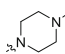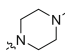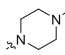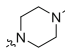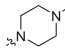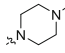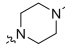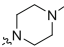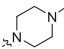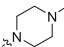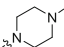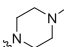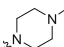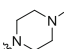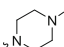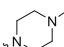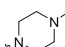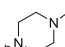
Comp.	R₁	R₄	R5′	R6′	pIC50		
					Exper	CoMFA	CoMSIA
17	H	NH₂	(structure)	H	7.54	7.64	7.45

Comp.	R₅′	R₅	R₆	R₇	R₈	pIC50		
						Exper	CoMFA	CoMSIA
18	(piperazine)	F	H	H	H	7.19	7.10	7.18
19*	(piperazine)	Cl	H	H	H	7.85	7.49	7.53
20	(piperazine)	CH₃	H	H	H	7.92	7.77	7.81
21	(piperazine)	MeNH	H	H	H	7.28	7.26	7.32
22*	(piperazine)	H	F	H	H	7.11	7.36	6.84
23	(piperazine)	H	Cl	H	H	7.37	7.23	7.41
24	(piperazine)	H	NH₂	H	H	7.72	7.74	7.84
25	(piperazine)	H	Me₂N	H	H	6.80	6.87	6.77

Table 1 continued

Comp.	R$_{5'}$	R$_5$	R$_6$	R$_7$	R$_8$	pIC50		
						Exper	CoMFA	CoMSIA
26		H	PhC(O)NH	H	H	6.01	6.10	6.00
27		H	BnNH	H	H	7.68	7.60	7.53
28		H	BnNHC(O)	H	H	7.30	7.37	7.25
29		H	H	F	H	7.85	7.70	7.77
30		H	H	MeNH	H	6.00	5.92	5.93
31		H	H	H	F	6.25	6.26	6.21
32		H	F	F	H	6.72	6.82	6.81
33*		F	H	F	H	6.89	7.16	6.51
34*		H	F	Me$_2$N	H	5.28	5.53	5.45
35	H		H	H	H	7.77	7.88	7.83
36	H	H		H	H	5.19	5.20	5.25

* Test set compounds

Fig. 1 Template used for molecular alignment (compound **20**)

Fig. 2 Superposition of all database alignment molecules

External validation

The internal validation of QSAR models used the LOO method, and the external validation was through the Q^2_{ext} (Golbraikh and Tropsha, 2002):

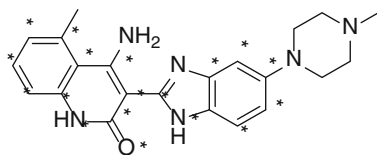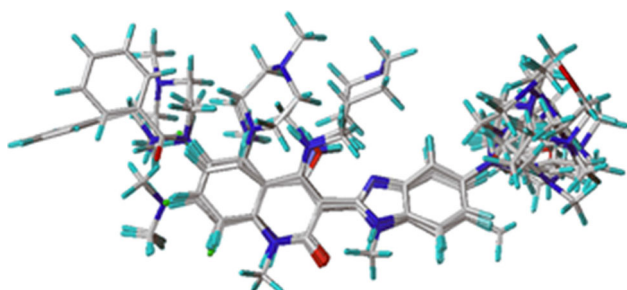$$Q^2_{ext} = 1 - \sum_{i=1}^{n} (y_i - \hat{y}_i)^2 / \sum_{i=1}^{n} (y_i - \overline{y}_{tr})^2.$$

In this equation, y_i is the observed activity (pIC$_{50}$) of test set, $\hat{y}_i$ is the predicted activity of test set, and $\overline{y}_{tr}$ is the mean values of observed activity of training set.

Molecular docking

The crystal structure of VEGFR-2 tyrosine kinase in complex with its inhibitor vandetanib (PDB ID: 2IVU) was recovered from the Protein Data Bank (http://www.rcsb.org/pdb/home/home.do). The docking studies were carried out with Autodock 4.2 (http://autodock.scripps.edu/) running on an Intel I7 computer under the Windows system. The receptor grids were generated by setting up the grid box on the center of co-crystalized ligand. Before docking all ligands and water molecules in 2IVU have been deleted, then the polar hydrogen atoms and charges were added to 2IVU.

Results and discussion

CoMFA and CoMSIA analysis

Often for QSARs developed with CoMFA, a shift in the q^2 values is observed as the grid spacing is altered. To examine this possibility with these data, the different grid boxes with 1.0, 1.5, 2.0, 2.5, and 3.0 Å grid spacing,

respectively, were used for the CoMFA calculations. The influence of the different grid spacings to CoMFA model is obvious. Only from the q^2 after leave-one-out cross-validation, the model with the grid spacing of 2.0 Å was selected as the best model.

The PLS statistics of the CoMFA analyses are summarized in Table 2. The cross-validated q^2 value was 0.516 with 3 components and non-cross-validated conventional R^2 value was 0.927 with a standard error of estimate (*SEE*) value of 0.207. The relative contribution between steric and electrostatic fields for the CoMFA model was 0.689 and 0.311, respectively, indicating that steric field is more predominant.

The CoMSIA analysis was performed using three descriptor fields: steric, electrostatic, and hydrophobic. Statistically significant CoMSIA model was obtained using the combination of steric, electrostatic, and hydrophobic fields ($q^2 = 0.538$, $R^2 = 0.980$, $F = 144.675$, $SEE = 0.131$). As obvious from Table 2, the corresponding field contributions are 0.379, 0.457, and 0.164, respectively.

To test the stability and predictive ability of the 3D-QSAR model, nine compounds, which were not included in the 3D-QSAR model, were selected as a set for validation. The predicted pIC50 for this test set is listed in Table 1. With the CoMFA model, the external cross-validated value (Q^{2}ext) was 0.855; with the CoMSIA model, the Q^{2}ext value was 0.809. The correlation between the experimental and predicted pIC$_{50}$ for training set is shown in Fig. 3. It was shown that the CoMFA and CoMSIA models were stable and had robust predictive ability.

Analysis of contours for CoMFA models

The CoMFA steric and electrostatic fields from the non-cross-validated analysis were plotted as three-dimensional colored contour maps in Fig. 4. To aid visualization, the most potent compound **20** was overlaid on the map.

Table 2 PLS Statistics of CoMFA and CoMSIA 3D-QSAR Models

PLS statistics	CoMFA	CoMSIA
N	3	5
q^2	0.516	0.538
R^2	0.927	0.980
F	135.478	144.675
SEE	0.207	0.131
Steric	0.689	0.379
Electrostatic	0.311	0.457
Hydrophobic	–	0.164

N is the number of components from PLS analysis, q^2 is the correlation coefficient of the leave-one-out (LOO) cross-validation, R^2 is the non-cross-validation coefficient, *F* is the Fischer ratio, and *SEE* is the standard deviation of the regression, respectively
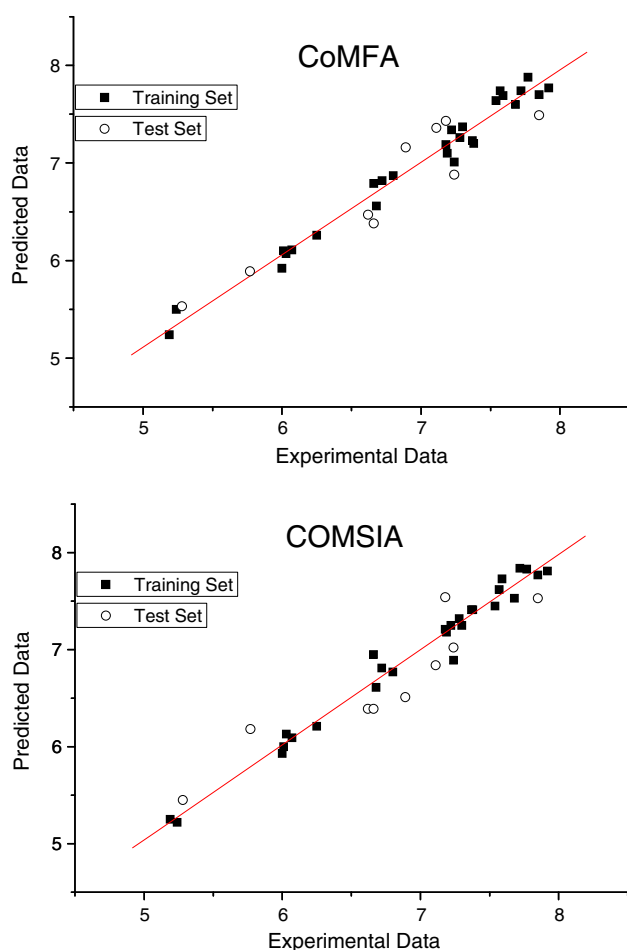
Fig. 3 Plots of the experimental and calculated pIC$_{50}$ for CoMFA and CoMSIA analysis

CoMFA steric contour maps are shown in Fig. 4a. In the steric fields, sterically favorable areas are shown in green and sterically unfavorable areas are shown in yellow. A large green contour at the 5′ position of the benzimidazole ring indicates that a sterically bulky group is favored in this

region. This may be the reason why compounds with 1-methylpiperazine moiety or methylene-extended amine substituents in this area, e.g., compounds 16 and 18–34, are more potent than molecules without any substituent at this particular position, such as compounds 1–7, 35, and 36. Additionally, the contour plot shows a yellow polyhedron in the left corner of Fig. 4a. The yellow region indicates that bulky substituent at this position might decrease the biological activity. CoMFA electrostatic contour maps are shown in Fig. 4b. Similarly, in the electrostatic fields, the electron-donating groups are favorable in blue regions and the electron-withdrawing groups are favorable in red regions. A red contour on the left side of the image indicates that an electron-withdrawing group at this position can improve inhibitory activity, as exemplified by comparing compounds 11 and 19.

Considering the analysis from steric field, it is concluded that the 5′ positions of the benzimidazole ring favor big and electron-withdrawing groups.

Analysis of the contours for CoMSIA models

The CoMSIA contours maps, derived using steric, electrostatic, and hydrophobic fields are presented in Fig. 5. CoMSIA steric and electrostatic contours more or less similar to those of the CoMFA are displayed in Fig. 5a, b. In the CoMSIA hydrophobic fields, hydrophobic favorable areas are shown in yellow and hydrophobic unfavorable areas are shown in white.

As shown in Fig. 5c, a large hydrophobic region (yellow) with two contours appears running from pyridine to the chlorobenzene ring and a small hydrophilic area (white) with three small polyhedrons appears around the fourth position of phenyl ring, and the most potent compounds each have a hydrophobic substituent. For the least active compound, the absence of chlorine leads to a weak activity.
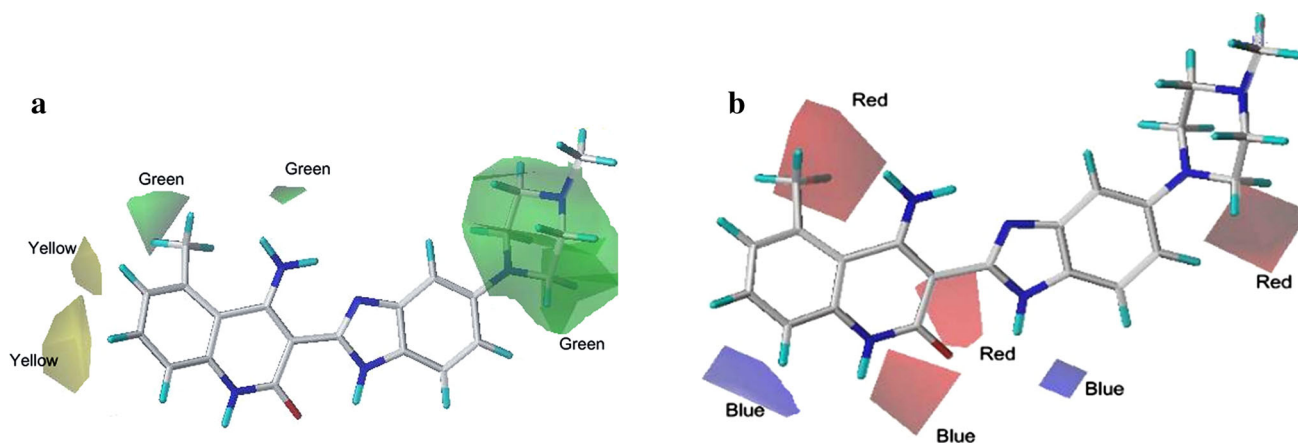

Fig. 4 Contour plots of CoMFA analysis in combination with compound **20**. **a** Steric Field; **b** Electrostatic Field
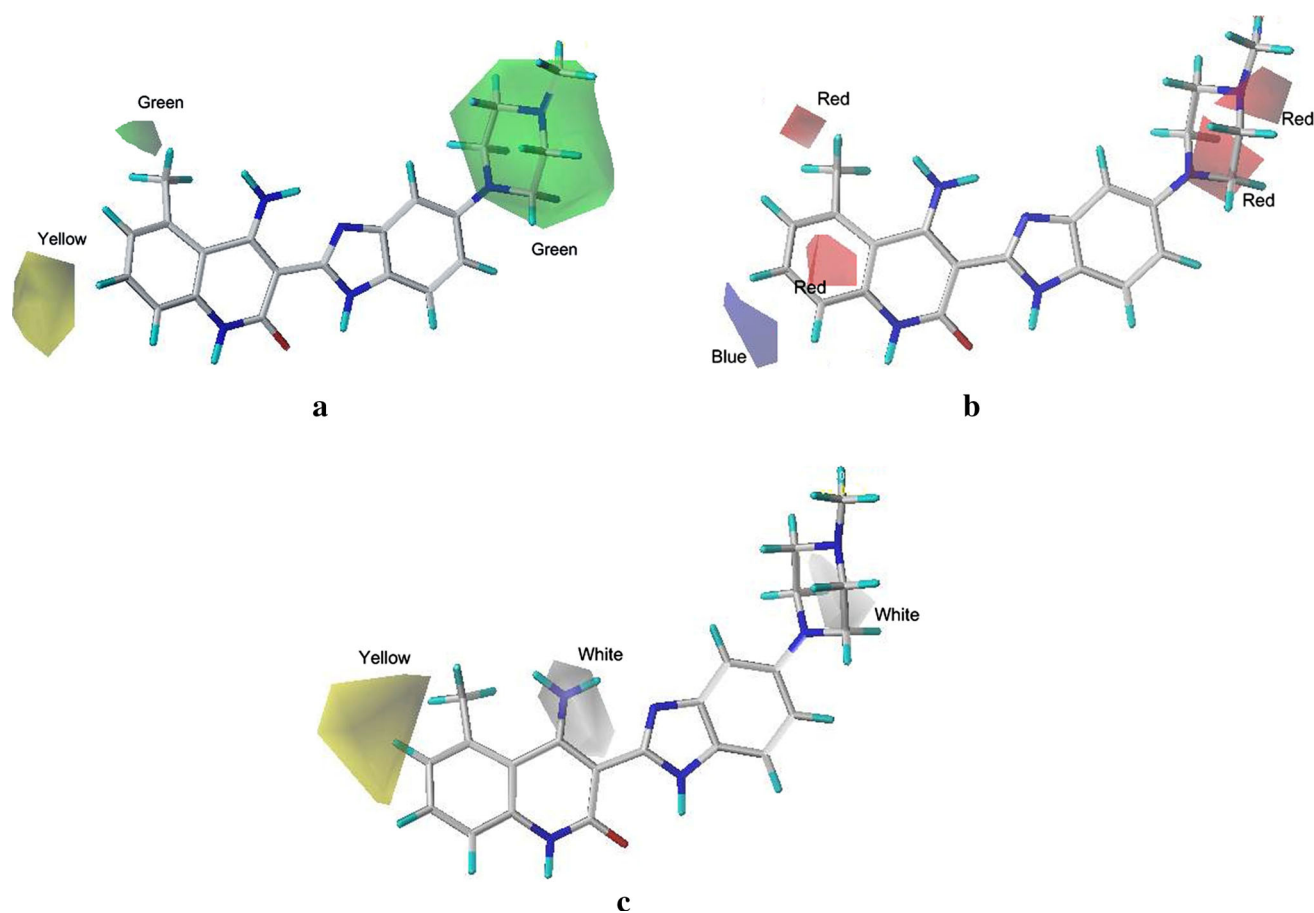
Fig. 5 Contour plots of CoMSIA analysis in combination with compound **20**. **a** Steric Field; **b** Electrostatic Field; **c** Hydrophobic Field

Docking analysis

All the selected compounds were docked into the active site of the target protein using the same docking protocol. Compound **20**, the most active compound in the dataset, was used to investigate the binding mode of the 3-benzimidazol-2-ylhydroquinolin-2-one derivative inhibitors. Compound **20** binds to the VEGFR-2 tyrosine kinase active site with a conformation similar to that of the known vandetanib inhibitor (Knowles *et al.*, 2006).

As shown in Fig. 6, the quinolinone and benzimidazoles ring inserted into the end of the binding pocket, bulky substituents will decrease the potency because of the steric hindrance. The 5′ site of the benzimidazoles ring is at the start of the binding pocket, which exposes to solvents and should be bulky.

Design of new molecules based on 3D-QSAR and Docking Studies

According to the 3D-QSAR predictions, the chemical structures and predicted activities of seven molecules, which

were designed based on the conformation of the compound **20** are listed in Table 3. When the substituted groups become larger at 5′-positions, the activation of 3-benzimidazol-2-ylhydroquinolin-2-one derivatives increased markedly, which can be exemplified by comparing compounds 9 and
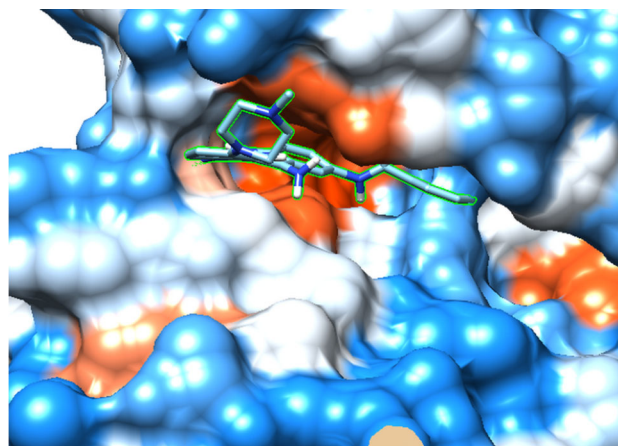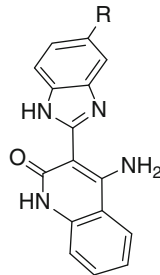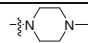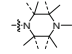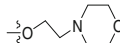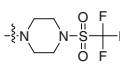

Fig. 6 The binding conformation of compound **20** with VEGFR-2 tyrosine kinase

Table 3 Structures, predicted pIC50 of the designed molecules compared to Compound **20**

No.	R	Predicted date	
		CoMFA	CoMSIA
20		7.90	7.85
D1		8.01	8.12
D2		7.94	7.99
D3		7.84	7.87
D4		7.92	7.91
D5		7.94	8.01
D6		7.99	7.88
D7		8.02	8.16

11. However, if 5′-substituted groups were too large, the activity will be decreased. When other substituents changed, the activation of 3-benzimidazol-2-ylhydroquinolin-2-one derivatives had inapparent changes.
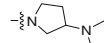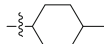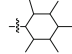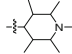
Conclusion

In this work, 3D-QSAR and molecular docking studies were carried out to explore the binding of 36 inhibitors to VEGFR-2 tyrosine kinase, and to construct highly predictive 3D-QSAR models for designing new VEGFR-2 tyrosine kinase inhibitors for the treatment of various angiogenic-related disorders. The predictive abilities of CoMFA and CoMSIA have been showed by the external validation (Q^2ext), which also been confirmed by molecular docking. For the 3-benzimidazol-2-ylhydroquinolin-2-one derivatives, the 5′-site should be bulky. Based on the 3D-QSAR and docking results, some potential candidates with high predictive biological activities have been found. This study can be served as a useful guideline for further modification of 3-benzimidazol-2-ylhydroquinolin-2-one derivatives which function as VEGFR-2 tyrosine kinase inhibitors.

References

Bhargava P, Robinson MO (2011) Development of second-generation VEGFR tyrosine kinase inhibitors: current status. Curr Oncol Rep 13:103–111

Böhm M, Stürzebecher J, Klebe G (1999) Three-dimensional quantitative structure-activity relationship analyses using comparative molecular field analysis and comparative molecular similarity indices analysis to elucidate selectivity differences of inhibitors binding to trypsin, thrombin, and factor Xa. J Med Chem 42:458–477

Bush BL, Nachbar RB Jr (1993) Sample-distance partial least squares: PLS optimized for many variables, with application to CoMFA. J Comput Aided Mol Des 7:587–619

Cai Z, Wei D, Borzilleri RM, Qian L, Kamath A, Mortillo S, Wautlet B, Henley BJ, Jeyaseelan R Sr, Tokarski J, Hunt JT, Bhide RS, Fargnoli J, Lombardo LJ (2008) Synthesis, SAR, and Evaluation of 4-[2,4-Difluoro-5-(cyclopropylcarbamoyl)phenylamino]pyrrolo[2,1-f][1,2,4]triazine-based VEGFR-2 kinase inhibitors. Bioorg Med Chem Lett 18:1354–1358

Carmeliet P (2000) Mechanisms of angiogenesis and arteriogenesis. Nat Med 6:389–398

Clark M, Cramer RD, Van Opdenbosch N (1989) Validation of the general purpose Tripos 5.2 force field. J Comput Chem 10:982–1012

Cramer RD III (1993) Partial least squares (PLS): its strengths and limitations. Perspect Drug Discov Des 1:269–278

Cramer RD, Patterson DE, Bunce JD (1988) Comparative molecular field analysis (CoMFA). 1. Effect of shape on binding of steroids to carrier proteins. J Am Chem Soc 110:5959–5967

Ding L, Tang F, Huang W, Jin Q, Shen H, Wei P (2013) Design, synthesis, and biological evaluation of novel 3-pyrrolocyclohexylene-2-dihydroindolinone derivatives as potent receptor tyrosine kinase inhibitors. Bioorg Med Chem Lett 23:5630–5633

Doi T, Ohtsu A, Fuse N, Yoshino T, Tahara M, Shibayama K, Takubo T, Weinreich DM (2013) Phase 1 study of trebananib (AMG 386), an angiogenesis targeting angiopoietin-1/2 antagonist, in Japanese patients with advanced solid tumors. Cancer Chemother Pharmacol 71:227–235

Golbraikh A, Tropsha A (2002) Beware of q2. J Mol Graph Model 20:269–276

Gupta N, Vyas VK, Patel B, Ghate M (2014) Predictive 3D-QSAR and HQSAR model generation of isocitrate lyase (ICL) inhibitors by various alignment methods combined with docking study. Med Chem Res 23:2757–2768

Jeltsch M, Leppänen V, Saharinen P, Alitalo K (2013) Receptor Tyrosine Kinase-Mediated Angiogenesis. Cold Spring Harb Perspect Biol 5:a9183

Klebe G, Abraham U, Mietzner T (1994) Molecular similarity indices in a comparative analysis (CoMSIA) of drug molecules to correlate and predict their biological activity. J Med Chem 37:4130–4146

Knowles PP, Murray-Rust J, Kjær S, Scott RP, Hanrahan S, Santoro M, Ibáñez CF, McDonald NQ (2006) Structure and chemical inhibition of the RET tyrosine kinase domain. J Biol Chem 281:33577–33587

Lee JS, Hirsh V, Park K, Qin S, Blajman CR, Perng R, Chen Y, Emerson L, Langmuir P, Manegold C (2012) Vandetanib versus placebo in patients with advanced non–small-cell lung cancer after prior therapy with an epidermal growth factor receptor tyrosine kinase inhibitor: a randomized, double-blind phase III trial (ZEPHYR). J Clin Oncol 30:1114–1121

McIntosh AR, Bookstein FL, Haxby JV, Grady CL (1996) Spatial pattern analysis of functional brain images using partial least squares. Neuroimage 3:143–157

Ramsden JD (2000) Angiogenesis in the thyroid gland. J Endocrinol 166:475–480

Renhowe PA, Pecchi S, Shafer CM, Machajewski TD, Jazan EM, Taylor C, Antonios-McCrea W, McBride CM, Frazier K, Wiesmann M (2009) Design, structure–activity relationships and in vivo characterization of 4-amino-3-benzimidazol-2-ylhydroquinolin-2-ones: a novel class of receptor tyrosine kinase inhibitors. J Med Chem 52:278–292

Shibuya M (2013) Vascular endothelial growth factor and its receptor system: physiological functions in angiogenesis and pathological roles in various diseases. J Biochem 153:13–19

Steeghs N, Gelderblom H, Wessels J, Eskens FA, de Bont N, Nortier JW, Guchelaar H (2011) Pharmacogenetics of telatinib, a VEGFR-2 and VEGFR-3 tyrosine kinase inhibitor, used in patients with solid tumors. Invest New Drugs 29:137–143

Viswanadhan VN, Ghose AK, Revankar GR, Robins RK (1989) Atomic physicochemical parameters for three-dimensional structure directed quantitative structure-activity relationships. 4. Additional parameters for hydrophobic and dispersive interactions and their application for an automated superposition of certain naturally occurring nucleoside antibiotics. J Chem Inf Comput Sci 29:163–172

Wold S, Sjöström M, Eriksson L (2001) PLS-regression: a basic tool of chemometrics. Chemometr Intell Lab 58:109–130

Xiao A, Zhang Z, An L, Xiang Y (2008) 3D-QSAR and docking studies of 3-arylquinazolinethione derivatives as selective estrogen receptor modulators. J Mol Model 14:149–159